Renewable Energy 101 (2017) 1299–1310

Contents lists available at ScienceDirect

Renewable Energy

journal homepage: www.elsevier.com/locate/renene

Identification of unknown parameters of a single diode photovoltaic model using particle swarm optimization with binary constraints

Sangram Bana*, R.P. Saini

Alternate Hydro Energy Centre, Indian Institute of Technology, Roorkee, 247667, India

ARTICLE INFO

Article history:
Received 31 March 2016
Received in revised form
13 August 2016
Accepted 4 October 2016
Available online 8 October 2016

Keywords:
Photovoltaic (PV) model
Maximum power point (MPP)
Binary constraints
Particle swarm optimization (PSO)

ABSTRACT

Abstract-Photo-voltaic (PV) is a static medium to convert solar energy directly into electricity. In order to predict the performance of a PV system before being installed, a reliable and accurate model design of PV systems is essential. To validate the design of a PV system like maximum power point (MPP) and micro-grid system through simulation, an accurate solar PV model is required. However, information provided by manufacturers in data sheets is not sufficient for simulating the characteristic of a PV module under normal as well as under diverse environmental conditions. In this paper, a particle swarm optimization (PSO) technique with binary constraints has been presented to identify the unknown parameters of a single diode model of solar PV module. Multi-crystalline and mono-crystalline technologies based PV modules are considered under the present study. Based on the results obtained, it has been found that PSO algorithm yields a high value of accuracy irrespective of temperature variations.

1. Introduction

In the current scenario, socio-economic development and human welfare around the world depends on energy. Fossil fuels account maximum share in the overall generation. However, carbon emissions and depletion are some issues associated with the use of fossil fuels. The energy demand around the world is continuously increasing. If this escalating demand is to be met with fossil fuels, the extensive use of fossil fuels will release a large amount of CO_2 and other greenhouse gases. Renewable energy sources on the other hand are abundant in nature and contain quite low or no greenhouse-gas emissions. Therefore, it is the necessity of today's world to concentrate on renewable energy sources for electricity generation. Solar energy has been a paramount part of renewable energy sources as it is available directly from the sun, whereas wind, wave, hydro etc. are indirectly derived. Solar energy is also available in abundance and is non exhaustible, but the technology to harness solar energy is still improving. Solar PV technology exploits the solar radiation and directly converts it into electricity. The utilization of photovoltaic (PV) technology as a source of power at user end is increasing, due to easy implementation and low maintenance cost compared to other forms of energy conversion [1]. PV technology has the highest power density amongst all renewable energy resources with global mean of 170 W/m^2 [2]. In order to predict the performance of a PV system, a reliable and accurate model design of PV systems is a necessary before being installed.

Performance of the PV system is affected by change in temperature and insolation [3]. Ideally a PV module needs to be operated at maximum power point (MPP). This incorporates advance research in real time optimization techniques like fuzzy logic, artificial neural network, perturb and observe algorithms etc. [4]. Therefore, it is essential to have a comprehensive study and performance analysis of a PV model to predict the outcome of a PV module under diverse atmospheric conditions.

The parameters provided in the manufacturers datasheet under standard test conditions (STC) include short-circuit current, open-circuit voltage, voltage at maximum power, current at maximum power and temperature coefficients of current, voltage and power. Although, provided data is essential but not enough to predict accurate I-V characteristic curves under varying insolation and temperature levels. Single diode PV model is extensively used by several researchers [5–9,11,12,45–47] due to its simplicity. Humada et al. [12] compared and summarizes the techniques for parameter extraction. Further, they have also compared single-diode and double diode models for one, two, three, four and five parameters by setting a model evaluation criterion. The study suggests that five parameter (single-diode) model is the most widely model due to its

* Corresponding author.
E-mail address: sonamdah@iitr.ac.in (S. Bana).

http://dx.doi.org/10.1016/j.renene.2016.10.010
0960-1481/

Nomenclature

a_{min}	minimum value of ideality factor
a_{max}	maximum value of ideality factor
b	index of the best individual in population
c_1 and c_2	acceleration factor
D	component of each individual of population
$f(.)$	objective function to be evaluated
F^k_i	value of objective function for ith individual of population at iteration k
$\mathbf{Gbest}^k$	the global best individual of population up to iteration k
$Gbest^k_j$	j^{th} component of the best individual of population up to iteration k
i	individuals of population i$\in$ {1, 2,…, N}
j	components of an individual j $\in$ {1, 2,…, D}
k	iteration counter (k $\in$ {1, 2,…, Maxite})
Maxite	maximum number of iterations
N	population size
$\mathbf{Pbest}^k_i$	personal best of ith individual of population up to iteration k
$Pbest^k_{i,j}$	personal best jth component of ith individual of population up to iteration k
$rand(\ )$	uniformly generated random number in the range[0, 1]
$R_{s\ min}$	minimum value of series resistance factor
$R_{s\ max}$	maximum value of series resistance factor
$R_{p\ min}$	minimum value of shunt resistance factor
$R_{p\ max}$	maximum value of shunt resistance factor
$Sign(.)$	signum function on each variable of the input vector
$\mathbf{V}$	initial velocity of N individuals each having D components
$V^k_{i,j}$	velocity of jth component of ith individual of population at iteration k
$\mathbf{X}$	population of N individuals each having D components (variables)
$\mathbf{X}^k_i$	i^{th} individual of population X at iteration k, i.e., $X^k_i = [X^k_{i,1}, X^k_{i,2},\ldots, X^k_{i,D}]$
ω	inertia factor
ω_{max}	maximum value of inertia factor
ω_{min}	minimum value of inertia factor

Abbreviations

ABSO	Artificial Bee Swarm optimization
BFA	Bacteria foraging algorithm
CPSO	Chaos particle swarm optimization algorithm
CSA	Cuckoo Search algorithm
EAs	Evolutionary algorithms; *GA* Genetic algorithm; *MAE* Mean absolute error; *MPP* Maximum power point; *MPPT* Maximum power point tracking; *PSO* Particle swarm optimization; *PV* Photo-voltaic; *RMSE* Root mean square error; *SA* Simulated annealing; *STC* Standard test conditions

high accuracy and less complex design.

The main issue associated with single-diode PV model is to identify five unknown parameters i.e. ideality factor (a), series resistance (R_s), shunt resistance (R_p), reverse saturation current (I_o) and photovoltaic current (I_{pv}). Identification of these parameters by a suitable method is essential in order to accurately predict the PV module characteristics. The methods include analytical approach, iterative approach or real time approach.

Studies have been carried out using an ideal model of a PV cell which does not include series and shunt resistance [13,14] as shown in Fig. 1.

The previous studies suggested that ideal model is simple but less accurate. Researchers in Refs. [10,15–18] proposed models with four parameters (a, R_s, I_o, I_{pv}) accounting shunt resistance to be infinite. Although, the proposed four parameters model has not been proved accurate yet, it is considered to be favorable as the unknown parameters can be easily identified in comparison to the model with five parameters (a, R_s, R_p, $I_o$and I_{pv}).

To resolve the issue with the necessity of obtaining unknown parameters, a five parameter model based on the values of manufacturer datasheet was presented by Villalva et al. [19]. Value of ideality factor was obtained through trial and error method. The

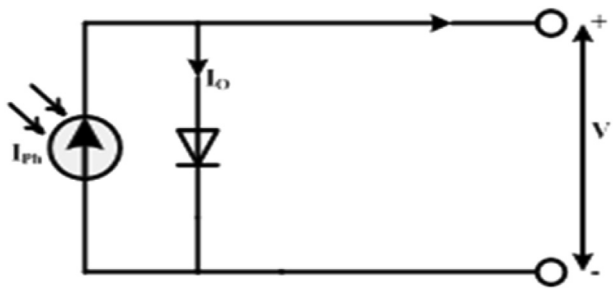

Fig. 1. Equivalent circuit of an ideal PV model.

new value of R_s and R_p depends upon the previous value of R_s. The new set of values was determined by continuously increasing R_s and simultaneously computing R_p. These values were determined till MPP of the presented model reaches to the same value as provided in manufacturer's datasheet at STC. Once unknown parameters are extracted, these parameters are fixed and again calculated for same model under the influence of varying insolation and temperature levels. Under standard test conditions (STC), the developed method yields accurate MPP. However accuracy gets compromised under the effect of varying temperature [20].

W. Xiao et al. [21] used a database of MPP acquired from manufacturer in order to produce exact MPP at varying temperatures. At different values of temperature, MPP was matched by regulating ideality factor through iterative technique. The drawback associated herewith is to obtain the availability of MPP for varying temperatures, which is not provided in manufacturer datasheet. Park and Choi [22] employed a parameter extraction method based on datasheet values. MPP error formulation is incorporated as objective function and parameter optimization is achieved by using pattern search algorithm.

Recently numerous evolutionary algorithms (EAs) were adopted to determine unknown parameters of a PV module under consideration. Jena and Ramana [23] presented a critical review based on modeling and parameter identification of a PV cell for simulation. They have analyzed R_s, R_p and two diode model along with different parameter identification schemes (analytical as well as soft computing). In recent years, the metaheuristic optimization algorithms such as genetic algorithm (GA) [24–26], simulated annealing (SA) [27], artificial Bee Swarm optimization (ABSO) algorithm [28,29], and particle swarm optimization (PSO) [30], have received considerable attention towards solar cell parameters identification problem. Metaheuristic algorithms are appropriate selections for resolving the drawback associated with parameter extraction at varying atmospheric conditions.

In case of GA, serious shortcomings, namely low speed and

degradation for highly interactive fitness function has been reported [31,32]. El-Naggar et al. [27] employed Simulated Annealing (SA) to extract the parameters of single and two-diode models for cell and module. The trade-off between the cooling schedule and initial temperature is the major issue that makes SA a less preferable choice. Jieming et al. [33] utilized Cuckoo Search algorithm (CSA) to identify the parameters of the conventional and an advanced form of the single diode model for PV cell and module. Askarzadeh and Rezazadeh [34] employed ABSO to obtain the parameters of the single and double-diode models for PV module. Rajasekar et al. [35] presented a Bacteria Foraging algorithm (BFA) to compute all parameters of the single diode R_P-model under varying operating temperature and insolation values. By utilizing parameters provided on the manufacturer's datasheet, I_{pv} and I_0 were analytically computed, whereas a, R_s, and R_p were obtained by optimizing equation of slope at MPP.

Qin and Kimball [36] eliminated the idea of unknown parameters estimation for the SPV model. They exploited the field test data along with PSO algorithm to determine the value of a, R_s and R_p. Measurements of short circuit current and load data were required for the field test. Hengsi and Jonathan [30] employed PSO to extract PV cell parameters from the data measured under real operating conditions of varying insolation and temperature. Wei H et al. [37] used chaos particle swarm optimization algorithm (CPSO) to obtain unknown parameters of the single diode R_p model for a module. In CPSO, the chaotic search mechanism is utilized to re-initiate the stationary particles-causing an enhanced local and global search capability. Ye et al. [38] utilized PSO to determine the cell parameters of the single and two-diode models from the I–V curves. In comparison to GA, PSO was found to be more accurate with better computational speed. On the basis of operating conditions, module technology and type of model researchers have employed numerous parameter extraction techniques having advantages and disadvantages of their own. Among all the techniques, performance of PSO algorithm is found to have an adequate sense of balance between accuracy, speed and complexity.

The PSO algorithm is a swarm intelligence optimization algorithm based on observations of the social behavior of bird flocking or fish schooling [28–30,36–41]. Several authors have utilized and improved many versions of PSO algorithm [28,29,38–41]. However, every version of PSO has different advantage for different complex optimal problem. The major disadvantages observed in PSO are of premature convergence and the loss of diversity in the population.

In order to eliminate the mentioned disadvantage, a novel technique has been presented in this study to compute the unknown parameters (a, R_s and R_p) of a single diode PV model. In the present study, a PSO based single diode model is developed to predict unknown parameters under varying operating conditions. In order to retain these parameters within realistic ranges and considering the effects of temperature variation, a binary constraint has been imposed i.e. by penalizing the objective function when the solution attempts to exceed the predefined parameters boundary limits. The accuracy of the model is assured irrespective of the temperature change.

The present study deals with identification of PV model using PSO with binary constraints. An overview of mathematical modeling framework of a PV model is presented and further, the problem formulation along with the proposed optimization technique is discussed. Results and performance validation of the proposed technique are discussed in detail. Further, the obtained results are compared with the results of other methods proposed in Refs. [16] and [19]. The proposed technique is found to be advantageous as it has the capability of determining ideality factor, series and shunt resistance simultaneously without the need of estimating ideality factor and field data measurements. Also, the extracted parameters are computed as a function of insolation and temperature.

2. Mathematical modeling framework of a PV module based on single diode model

2.1. Ideal PV cell model

An ideal PV cell is represented by photo-generated current (I_{pv}) which diverges from the ideal outcome due to electrical and optical losses [23,41]. Further, the effect of series and parallel resistance are not considered in this simplest PV model. Schematic for an ideal PV model is shown earlier in Fig. 1. Terminal current of an ideal model is represented by I-V characteristics and mathematically expressed as:

$$I = I_{pv} - I_d \tag{1}$$

The diode current (I_d) signifies diffusion and recombination current in quasi steady state regions of emitter and excess concentration regions of PN junction. This diode current is represented by Shockley equation as:

$$I_d = I_0\left\{e^{qV_d/aKT} - 1\right\} \tag{2}$$

where q is the charge of an electron (1.6×10^{-19}C), K is the Boltzmann constant (1.3805×10^{-23} J/K) T is temperature (K), I_0 is leakage current and V_d is the diode voltage.

The ideal mathematical model based on diode equation of Shockley and Queisser is expressed as:

$$I = I_{pv} - I_0\left(e^{qV_d/aKT} - 1\right) \tag{3}$$

Ideal solar PV cell does not consider the effect of internal resistance, thus fails to establish an accurate relationship between cell current and voltage.

2.2. Practical PV cell model

In order to achieve accurate results, a series resistance is introduced to the ideal PV cell model. Although this model is simple but it reveals deficiencies when subjected to temperature variations. To overcome this limitation, the model has been extended further by considering a shunt resistance and is termed as Practical PV cell. Thus, the practical single diode PV or five parameter (I_{pv}, I_0, a, R_s and R_p) model consists of current producer and a diode with series and shunt resistance as shown in Fig. 2 [4–12,42]. The characteristics I-V curve of a practical PV cell is shown in Fig. 3.

The series resistance signifies resistance (ohmic loss) offered to

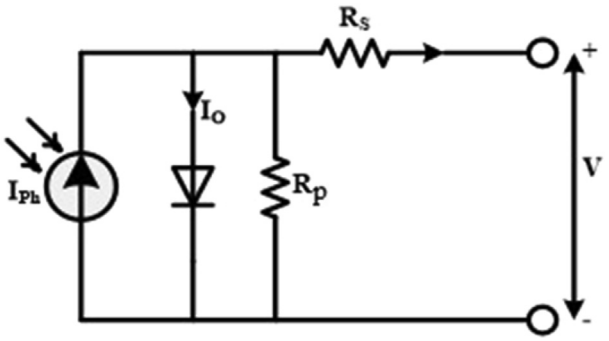

Fig. 2. Equivalent circuit of a practical PV cell.

the current flow due to ohmic contact (metal-semiconductor contact) and impurity concentrations along with junction depth. Leakage current across the junction signifies shunt resistance, connected parallel to the diode. The mathematical representation of terminal current in Eq. (1) is modified as:

$$I = I_{Pv} - I_d - V_d/R_p \tag{4}$$

$$V_d = V + IR_S \tag{5}$$

where V is input voltage and I is the terminal current.

It is recognized that I-V characteristic curve of a PV cell is affected by both series resistance and shunt resistance. The output voltage is affected by series resistance; while shunt resistance is responsible for reduction in available current [14,15,43–47]. Eq. (3) is modified to obtain the equation of single diode PV model. The terminal current of a single diode(five-parameter) model is given by:

$$I = I_{pv} - I_0\left[exp\left(\frac{V + IR_s}{aV_t}\right) - 1\right] - \frac{V + IR_s}{R_p} \tag{6}$$

where V_T is the thermal voltage (nkT/q).

2.3. Modeling of a PV module

A PV module may consist of number of PV cells which can be connected in series or parallel. This series-parallel topology is represented in Fig. 4.

The parameters of a PV cell are transformed in order to represent a PV module. Table 1 represents the parameters which are transformed due to series/parallel PV topologies [45,47].

Terminal current for series-parallel configuration of a PV module can be written as;

$$I = N_p\left\{I_{pv} - I_{s1}\left[exp\left(\frac{V + IR_s\left(\frac{N_s}{N_p}\right)}{aN_sV_t}\right) - 1\right]\right\} - \left\{\frac{V + IR_s\left(\frac{N_s}{N_p}\right)}{R_{sh}\left(\frac{N_s}{N_p}\right)}\right\} \tag{7}$$

A single PV module is a particular case of PV cells connected in series. Therefore, the number of cells connected in series (i.e. N_s) will be scaled with V_t. Now, Eq. (6) can be rewritten as;

$$I = I_{pv} - I_0\left[exp\left(\frac{V + IR_s}{aN_sV_t}\right) - 1\right] - \frac{V + IR_s}{R_p} \tag{8}$$

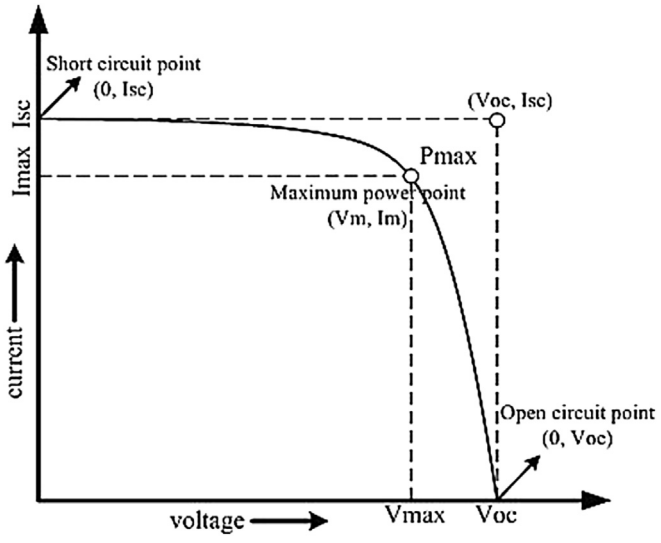

Fig. 3. I-V characteristics curve of a PV cell.

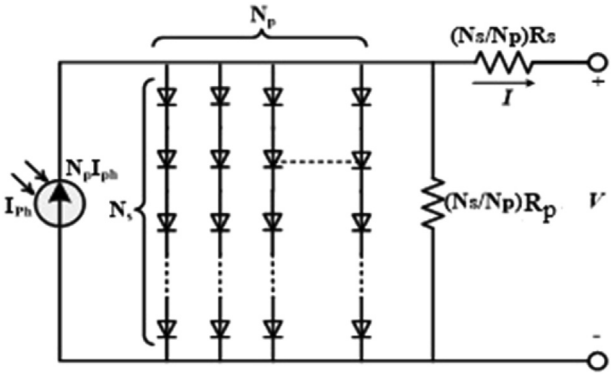

Fig. 4. Equivalent circuit model of a PV module.

Depending upon the load requirements, the numbers of modules are connected in series to increase voltage levels, whereas modules are connected in parallel to increase current levels.

When the terminals of a PV module are short-circuited, the current that flows through the circuit is termed as short-circuit current (I_{sc}). It is the maximum current that flows through a PV cell. I_{sc} of a PV module depends on incident insolation, which is determined by the spectrum of incident light, i.e. AM 1.5 spectrum. I_{sc} also depends on cell area and its ability to absorb incident solar radiation [23]. At a given temperature T, $V = 0$ and $I = I_{sc}$, Eq. (8) becomes:

$$I_{sc}(T) = \frac{R_p}{R_s + R_p}\left\{I_{pv} - I_0\left[exp\left(\frac{I_{sc}(T) + R_s}{aN_sV_t(T)}\right) - 1\right]\right\} \tag{9}$$

Open circuit voltage (V_{oc}) is the maximum voltage that can be delivered by a PV module. The Open circuit voltage corresponds to forward bias voltage, at which dark current compensates the photo-generated current and $V_{oc}$is dependent on the density of photo-generated current. At open circuit condition $I = 0$, $V = V_{oc}$ and Eq. (8) becomes;

$$V_{oc}(T) = R_p\left\{I_{pv} - I_0\left[exp\left(\frac{V_{oc}(T)}{aN_sV_t(T)}\right) - 1\right]\right\} \tag{10}$$

At a given temperature, maximum power is determined by the product of maximum current and voltage as shown in Fig. 3. By substituting $I = I_{mp}$ and $V = V_{mp}$, the maximum power at a given temperature can be determined from Eq. (8) as:

$$P_{mp}(T) = \frac{R_pV_{mp}(T)}{R_s + R_p} \times \left\{I_{pv} - I_0\left[exp\left(\frac{V_{mp}(T) + I_{mp}(T)R_s}{aN_sV_t(T)}\right) - 1\right] - \frac{V_{mp}(T)}{R_p}\right\} \tag{11}$$

Eqs. (9)–(11) are the data points used by the optimizer to provide the finest set of values for a, R_p and R_s. Also, the proportional effect of insolation intensity (G) and operating temperature (T) on the PV output current are given in Eqs. (9–11) [10,13–15,42–47].

The insolation dependence of PV current is given by;

Table 1
Transformed parameters for series and parallel topologies.

S.No.	Parameters of SPV cell	Parameters of PV module (N_S cells connected in series)	Parameters of PV module (N_p cells connected in parallel)
1.	I_{Pv}	I_{Pv}	N_pI_{Pv}
2.	V_t	N_sV_t	V_t
3.	R_s	N_sR_s	R_s/N_p
4.	R_{sh}	N_sR_{sh}	R_{sh}/N_p

$$I_{pv}(G,T) = \frac{G}{G_n}\left(I_{pv,n} + K_{I_{sc}}\Delta_T\right) \quad (12)$$

Where $I_{pv,n}$ is PV current and G_n is the solar radiation intensity in W/m^2 at STC under nominal conditions, K_{Isc} is the temperature coefficient of short circuit current (mA/°C) and ΔT ($= T - T_n$) is the difference of temperature between the present moment and STC.

2.4. Effect of temperature

Solar cells work best at low temperature as determined by their material properties. The cell efficiency decreases as the temperature escalates above operating temperature. A substantial part of incident insolation is lost in the form of heat resulting in high temperature of cells. To determine the effect of temperature on maximum power, $P_{mpp,e}(T)$, open circuit voltage, $V_{oc,e}(T)$ and short circuit current, $I_{sc,e}(T)$at a given temperature are expressed as;

$$I_{sc,e}(T) = I_{sc,n} + K_{I_{sc}}\Delta_T \quad (13)$$

$$V_{oc,e}(T) = V_{oc,n} + K_{V_{oc}}\Delta_T \quad (14)$$

$$P_{mp,e}(T) = P_{mp,n} + K_{P_{mp}}\Delta_T \quad (15)$$

where $P_{mpp,n}$, $V_{oc,n}$ and $I_{sc,n}$ respectively represents maximum power, open circuit voltage and short circuit current under nominal circumstances. K_{Voc} and K_{Pmp} are the temperature coefficient of open circuit voltage and maximum power point provided by the manufacturers as shown in Table 2. The datasheets of the considered modules are provided in Refs. [48,49] and [50].

The values of maximum voltage and maximum current temperature coefficient are not available and are approximated [47] as:

$$K_{V_{mp}} \approx K_{V_{oc}} \quad (16)$$

$$K_{I_{mp}} \approx K_{I_{sc}} \quad (17)$$

Therefore, at different temperatures values of V_{mp} and I_{mp} are anticipated as;

$$V_{mp}(T) = V_{mp,n} + K_{V_{oc}}\Delta_T \quad (18)$$

$$I_{mp}(T) = I_{mp,n} + K_{I_{sc}}\Delta_T \quad (19)$$

3. The proposed method and problem formulation

The PV model, represented in Eq. (8), is a mystical function which includes three unidentified parameters (a, R_s, and R_p). Conventional techniques like Newton–Raphson method triggers singularity due to large situation number of the Jacobin matrix. In order to overcome this drawback, a PSO based technique is considered and presented to eradicate the necessity for matrix inversion and partial differentiation.

3.1. Objective function

Based on the manufacture's data given in Table 2, the unidentified parameters of a single diode model as shown in Fig. 1 are to be identified in order to match the generated I-V and P-V curves of the presented model with the manufactures data at a specified temperature. The objective function for calculating PV module unknown parameters like ideality factor (a), series resistance (R_s) and parallel resistance (R_p) is defined as:

$$\min f_{obj} = |f_{Isc}| + |f_{Voc}| + |f_{Pmp}| \quad (20)$$

Contrasting the distinctive methodology that determines the model parameters by means of MPP only, the objective function in Eq. (20) consists of three data points [0, I_{sc}], [V_{mp}, I_{mp}] and [V_{oc}, 0] for optimization. It also contemplates the consequences of temperature on the PV module for identifying a, R_s and R_p in comparison to other techniques that are dependent on STC only.

To normalize the objective function, the numerator and denominator of equations from Eqs. (21)–(23) are obtained from Eqs. (9)–(11) and (13)–(15), respectively. This ensures that the range of the terms in the objective function is same.

Table 2
Parameters provided by the manufacturers of different PV modules at STC.

Parameters	Unit	Multi-crystalline	Mono-crystalline	Mono-crystalline
		Kyocera KD210GH-2PU	Shell SP70	Shell SQ85
I_{sc}	A	8.58	4.70	5.45
V_{oc}	V	33.20	21.40	22.20
I_{mp}	A	7.90	4.25	4.95
V_{mp}	V	26.60	16.50	17.20
K_{Voc}	(mV/°C)	−120	−76	−72.50
K_{Isc}	(mA/°C)	5.15	2	0.8
K_{Pmp}	(%/°C)	−0.45	−0.45	−0.43
N_s	Nos.	54	36	36

$$fI_{sc}(a, R_s, R_p, T) = \frac{I_{sc}(T)}{I_{sc,e}(T)} - 1 \quad (21)$$

$$fV_{oc}(a, R_s, R_p, T) = \frac{V_{oc}(T)}{V_{oc,e}(T)} - 1 \quad (22)$$

$$fP_{mp}(a, R_s, R_p, T) = \frac{P_{mp}(T)}{P_{mp,e}(T)} - 1 \quad (23)$$

3.2. Binary constraints handling approach

PV modules' parameters like ideality factor, series resistance and parallel resistance must be within their limits. Three set of constraints are imposed to handle this problem. The constraints are expressed as:

$$a_{\min} < a < a_{\max} \quad (24)$$

$$R_{s,\min} < R_s < R_{s,\max} \quad (25)$$

$$R_{p,\min} < R_p < R_{p,\max} \quad (26)$$

where the minimum and maximum values of the parameters to be determined are represented by the subscripts 'min' and 'max', respectively. The binary constraints considered for simulation are given in Table 3.

A binary constraint handling approach is proposed to penalize the objective function if any of the above constraint violates. The proposed approach for handling binary constraints is expressed as follows:

$$f_{barrier} = \Big[(sign(a_{\min} - a) + sign(a_{\max} - a))^2 + (sign(R_{s,\min} - R_s) + sign(R_{s,\max} - R_s))^2 + (sign(R_{p,\min} - R_p) + sign(R_{p,\max} - R_p))^2\Big] \quad (27)$$

where sign(x) is a function return as −1, 0 and 1 if x < 0, x = 0 and x > 0, respectively. This binary constraint handling approach is having advantages over the other constraints handling approach as it only penalizes the objective function if there is a constraint violation.

By introducing binary constraint handling approach term into the objective function, i.e., $f_{obj} = |f_{Isc}| + |f_{Voc}| + |f_{Pmp}| + |f_{barrier}|$, the problem is transformed into an unconstrained optimization problem.

The objective function given by Eq. (20) is minimized in order to determine a, R_s and R_p by formulating the PSO approach. In previous studies [37–39,45–50], PSO algorithm based technique has been used for maximization of the objective function. Whereas in the present study, the objective function is minimized to zero for different values of temperature and insolation using an absolute function.

3.3. PSO algorithm

Particle swarm optimization is inspired by social and cooperative behavior displayed by various species to fill their needs in the search space. The algorithm is guided by personal experience (Pbest), overall experience (Gbest) and the present movement of the particles to decide their next positions in the search space. Further, the experiences are accelerated by two factors c_1 and c_2 known as acceleration coefficients, and two random numbers generated between [0, 1], whereas the present movement is multiplied by an inertia factor 'ω' varying between [ω_{min}, ω_{max}]. The size of the population is considered as 'N' and the dimension of each element of the population is considered as D, where D represents the total number of variables. The initial solution is denoted as $\mathbf{X} = [\mathbf{X_1}, \mathbf{X_2} \ldots, \mathbf{X_N}]^T$, where 'T' denotes the transpose operator. Each individual $\mathbf{X}_i$ (i = 1, 2 … N) is given as $\mathbf{X}_i = [X_{i,1}, X_{i,2}, \ldots, X_{i,D}]$. The initial velocity of the population is denoted as $\mathbf{V} = [\mathbf{V_1}, \mathbf{V_2} \ldots, \mathbf{V_N}]^T$. Thus, the velocity of a particle $\mathbf{X}_i$ (i = 1, 2, …, N) is given as $\mathbf{V}_i = [V_{i,1}, V_{i,2}, \ldots, V_{i,D}]$.

The flowchart of the proposed PSO-based inverse barrier technique is shown in Fig. 5.

The different steps of PSO are as follows for ∀*I* and ∀*j* (where *'i'* represents particle and *'j'* its dimension):

Step 1. Set parameter ω_{min}, ω_{max}, c_1 and c_2 of PSO
Step 2. Initialize population of particles having positions **X** and velocities **V**
Step 3. Set iteration $k = 1$
Step 4. Calculate fitness of particles $F^k_i = f(\boldsymbol{X}^k_i)$ and find the index of the best particle b
Step 5. Select $\boldsymbol{Pbest}^k_i = \boldsymbol{X}^k_i$ and $\boldsymbol{Gbest}^k = \boldsymbol{X}^k_b$
Step 6. Take $\omega = \omega_{max} - k \times (\omega_{max} - \omega_{min})/Max_{iteation}$
Step 7. Update velocity and position of particles as;
$V^{k+1}_{i,j} = w \times V^k_{i,j} + c_1 \times rand(\,) \times (Pbest^k_{i,j} - X^k_{i,j}) + c_2 \times rand(\,) \times (Gbest^k_j - X^k_{i,j})$; ∀j and ∀i
$X^{k+1}_{i,j} = X^k_{i,j} + V^{k+1}_{i,j}$; ∀j and ∀i
Step 8. Evaluate fitness $F^{k+1}_i = f(\boldsymbol{X}^{k+1}_i)$ and find the index of the best particle b1
Step 9. Update Pbest of population
If $F^{k+1}_i < F^k_i$, then, $\mathbf{Pbest}^{k+1}_i = \mathbf{X}^{k+1}_i$ else $\mathbf{Pbest}^{k+1}_i = \mathbf{Pbest}^k_i$
Step 10. Update Gbest of population
If $F^{k+1}_{b1} < F^k_b$ then $\mathbf{Gbest}^{k+1} = \mathbf{Pbest}^{k+1}_{b1}$ and set b = b1 else $\mathbf{Gbest}^{k+1} = \mathbf{Gbest}^k$
Step 11. If $k <$ *Maxite* then $k = k + 1$ and go to step 6 else go to step 12
Step 12. Print optimum solution as $\boldsymbol{Gbest}^k$

Table 3
Binary constraints considered for simulation.

Parameters	Unit	Multi-crystalline	Mono-crystalline	Mono-crystalline
		Kyocera, KD210GH-2PU	Shell, SP70	Shell, SQ85
a_{min}	–	0.5	0.5	0.5
a_{max}	–	2.0	2.0	2.0
R_{Pmin}	ohm	0.001	0.001	0.001
R_{Pmax}	ohm	1.0	1.0	1.0
R_{Smin}	ohm	50	50	50
R_{Smax}	ohm	200	200	200

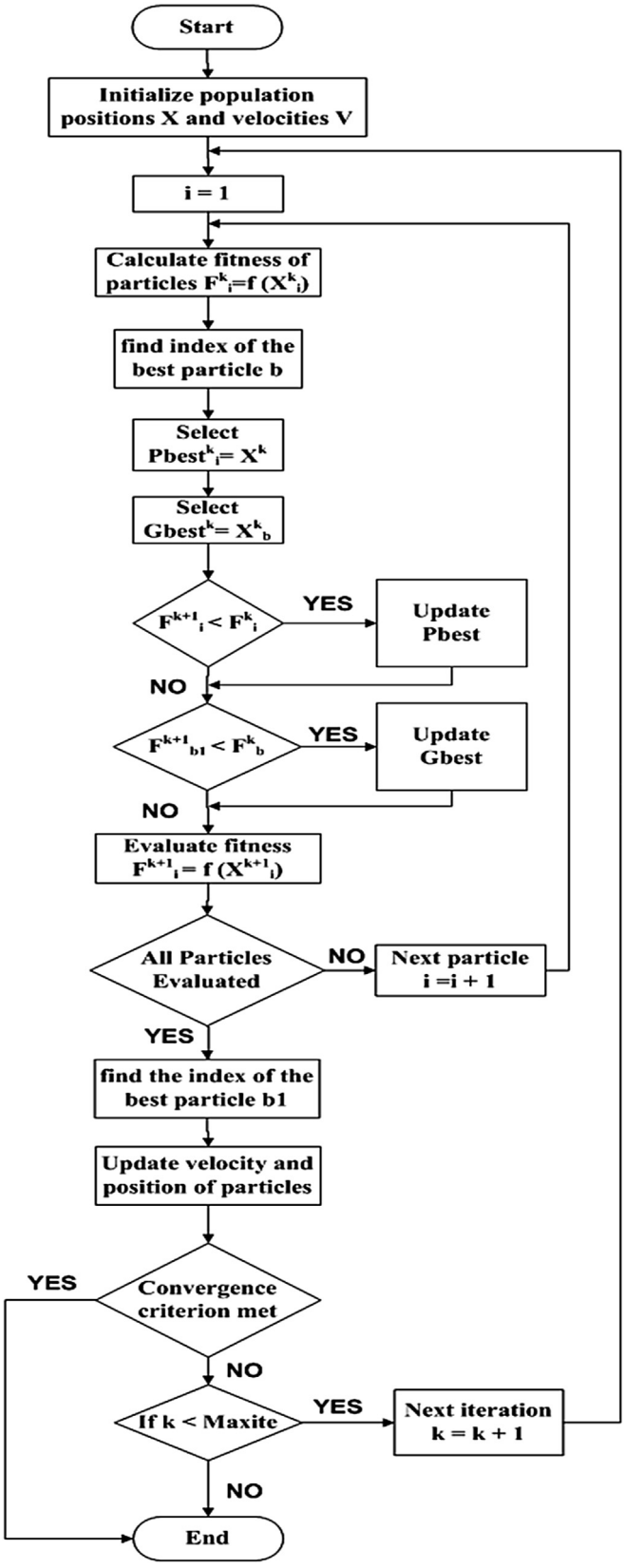

Fig. 5. Flowchart of the proposed technique.

Based on the randomly generated population, the PSO technique provides a collection of different solutions for a, R_s and R_p with each new execution of the optimization technique. This provides a set of I-V curves.

The technique provides several I-V and P-V curves as shown in Figs. 6 and 7 respectively that meet the objective function to confirm the authentication of the presented algorithm. The circle markers on these curves indicate $[0, I_{sc}]$, $[V_{mp}, I_{mp}]$ and $[V_{oc}, 0]$ which are the points that the I-V curve of the proposed method (indicated by the solid lines) must pass through.

The overall model error defined for each set of curves in Figs. 6 and 7 is represented by the following equation;

$$\varepsilon_i = \left|P_{mp,m_i}(T) - P_{mp,e}(T)\right| + \left|V_{mp,m_i}(T) - V_{mp,e}(T)\right| \quad (28)$$

Where ε is the overall model error and subscript i signifies the specific curve under assessment. From all the possible optimized solution, outcome with the least value of ε is selected as the best solution.

4. Results and discussions

Performance of the proposed optimization technique (PSO approach) has been investigated first. The parameters such as population size '*ps*' and acceleration coefficients c_1 and c_2 affect the execution of PSO. MATLAB environment is used to conduct this mathematical study. The parameters set up for considered PSO algorithm is shown in Table 4:

4.1. Convergence of PSO

In order to study the convergence of PSO for the proposed technique, PV modules of two different technologies have been used. As the temperature varies, for each value of temperature, PSO is implemented and gets terminated after 1000 generations. The optimization has been repeated for 100 times with some new sets of population in order to achieve the average of optimized results. Fig. 8 shows the best fitness value versus generations plot for different values of temperature.

The fitness value in curves converges to zero for SQ85 PV module irrelevant of the operating temperature. Similar results can be achieved for KD210GH-2PU and SP70 PV module. It is observed that after every 100 generations the fitness value drops down to zero in 8 ms of time to confirm the convergence of the fitness value.

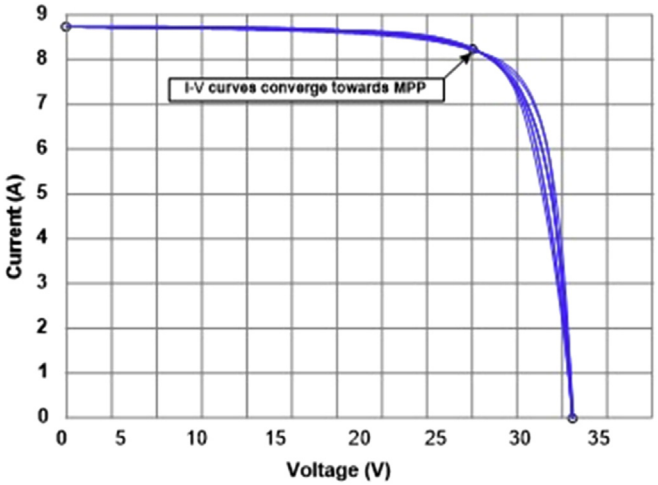

Fig. 6. I-V curves obtained by the presented technique.

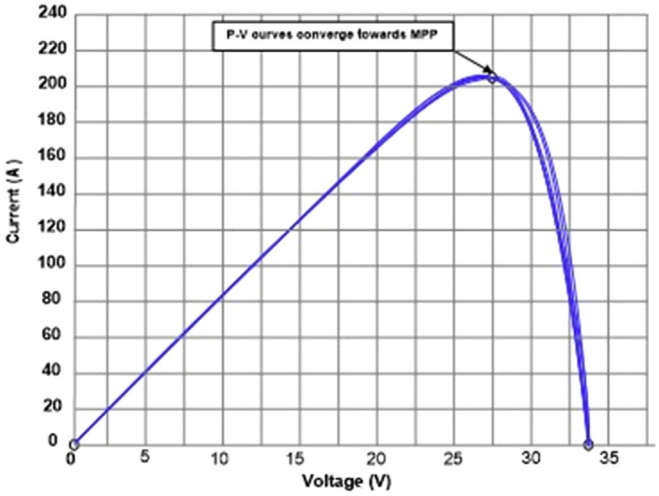

Fig. 7. P-V curves obtained by the presented technique.

Table 4
Parameters setup for considered PSO algorithm.

S.No.	Parameters	Values
1.	Population size (ps)	60
2.	Acceleration coefficients ($c_1 = c_2$)	2.0
3.	Minimum value of inertia factor, (ω_{min})	0.4
4.	Maximum value of inertia factor, (ω_{max})	0.9
5.	Maximum iteration	1000
6.	Maximum tolerance for objective function	10^{-8}

4.2. Model validation

Based on the convergence of the proposed algorithm, the PV modules of two different technologies are used to evaluate the proposed model under the present study. The parameters and constraints of these technologies are specified earlier in Tables 2 and 3, respectively. The identified parameters obtained by applying the proposed optimization technique are presented in Fig. 9.

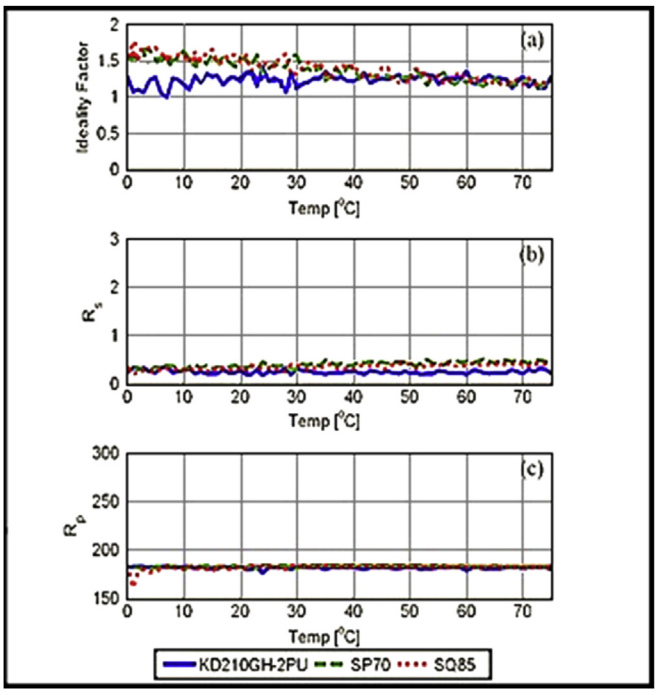

Fig. 9. Model parameters for KD210GH-2PU, SP70 and SQ85 at 0 °C to 75 °C. (a) Ideality factor. (b) Series resistance. (c) Shunt resistance.

Ideality factor, series resistance and shunt resistance for two different technologies (Mono-crystalline, KD210GH-2PU and Poly-crystalline, SP70 and SQ85 PV modules) have been extracted by the proposed technique for different values of temperature in the range of T = 0 °C–75 °C. Parameters exhibit non-linear characteristics and the ideality factor is on an urge of decrease [Fig. 9(a)]. On the other hand, series resistance shows escalating tendency [Fig. 9(b)] for SP70 and SQ85 PV modules. However, KD210GH-2PU PV module indicates the declining tendency in series resistance and inclining trend in ideality factor with increase in temperature. In

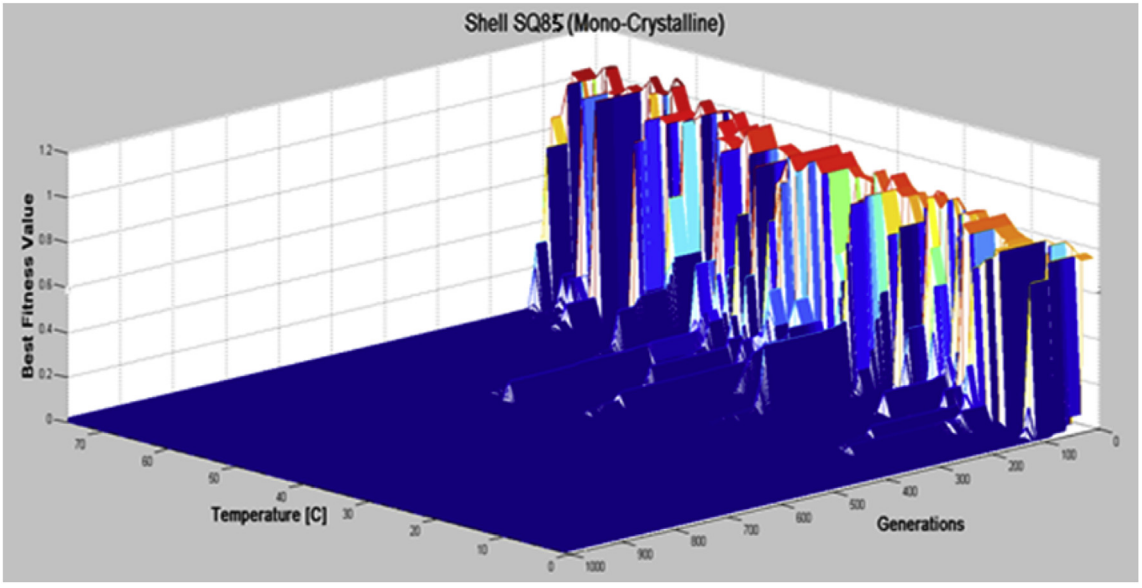

Fig. 8. Best fitness versus generations for T = 0 °C–75 °C for Shell SQ85.

Table 5
Identified parameters for KD210GH-2PU and SQ85 PV modules.

Temperature	Values	KYOCERA-KD210GH-2PU			SHELL-SQ85		
		a	R_s (Ω)	R_p (Ω)	a	Rs (Ω)	Rp (Ω)
25 °C	Best Value (G_{best})	1.6016	0.0012	104.5979	1.6056	0.0284	55.7392
	Mean Value (G_{mean})	1.4809	0.0909	142.7663	1.5603	0.2161	130.1744
	Worst Value (G_{worst})	0.6785	0.4989	193.9616	0.9177	0.5473	193.6260
50 °C	Best Value (G_{best})	1.5996	0.0010	199.9060	1.5998	0.0010	199.9962
	Mean Value (G_{mean})	1.5582	0.0186	165.0791	1.5448	0.0309	181.9622
	Worst Value (G_{worst})	0.5577	0.4393	107.2338	0.6785	0.4989	193.9616
75 °C	Best Value (G_{best})	1.5996	0.0010	199.9773	1.5998	0.0009	199.9274
	Mean Value (G_{mean})	1.5793	0.0099	158.1982	1.5726	0.0160	171.7543
	Worst Value (G_{worst})	0.5517	0.4393	107.2338	0.6786	0.4988	193.9616

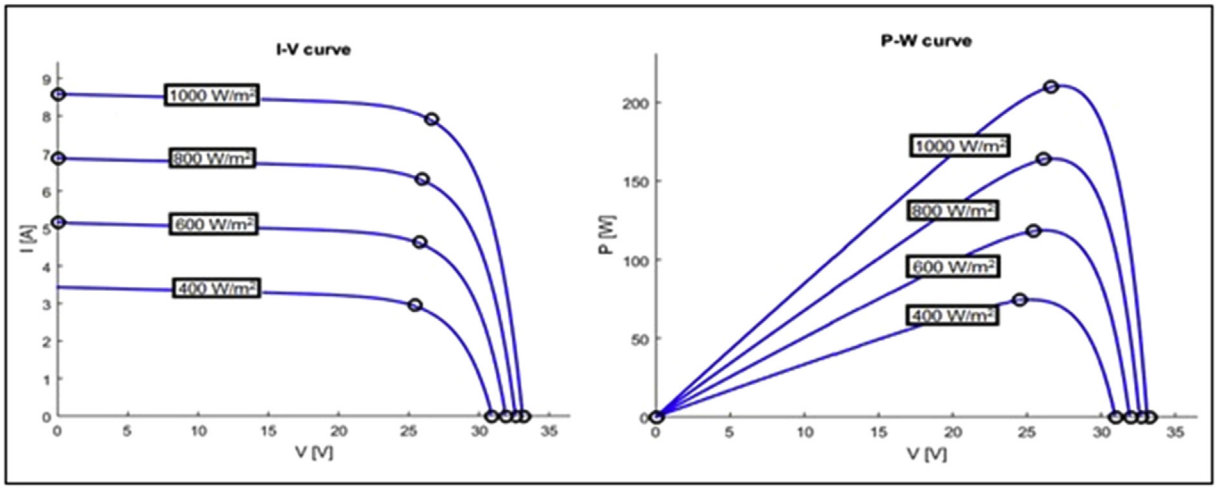

Fig. 10. I–V and P–V curves of proposed model (solid line) and manufacturer's experimental data (circle marker at I_{sc}, P_{mp} and V_{oc}) of KD210GH-2PU (Multi-crystalline) PV module under different irradiation, T = 25 °C.

case of shunt resistance, the values identified approximately remains constant for KD210GH-2PU, SP70 and SQ85 PV modules. Series resistance decreases with increase in the ideality factor and vice-versa. However, a slight variation has been observed in case of shunt resistance.

Out of 100 independent runs, the best value, mean value and worst value of ideality factor, series resistance and shunt resistance at different temperatures for KD210GH-2PU and SQ85 PV modules are presented in Table 5.

Based on the obtained values of the unknown parameters, I-V

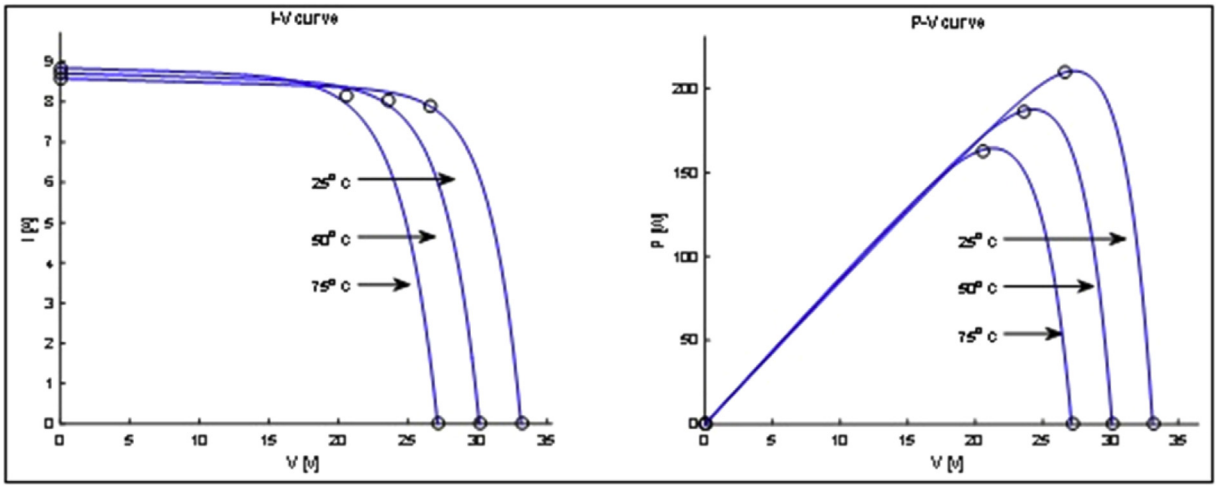

Fig. 11. I–V and P–V curves of proposed model (solid line) and manufacturer's experimental data (circle marker at I_{sc}, P_{mp} and V_{oc}) of KD210GH-2PU (Multi-crystalline) PV module at different temperature, G = 1000 W/m^2.

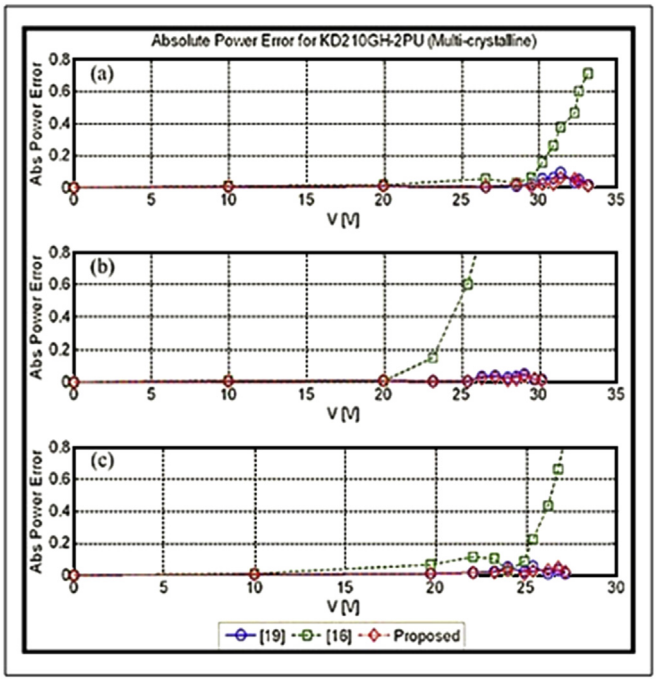

Fig. 12. Absolute power error for KD210GH-2PU (Multi-crystalline) at (a) T = 25 °C, (b) T = 50 °C, and (c) T = 75 °C, G = 1000 W/m^2, A.M = 1.5.

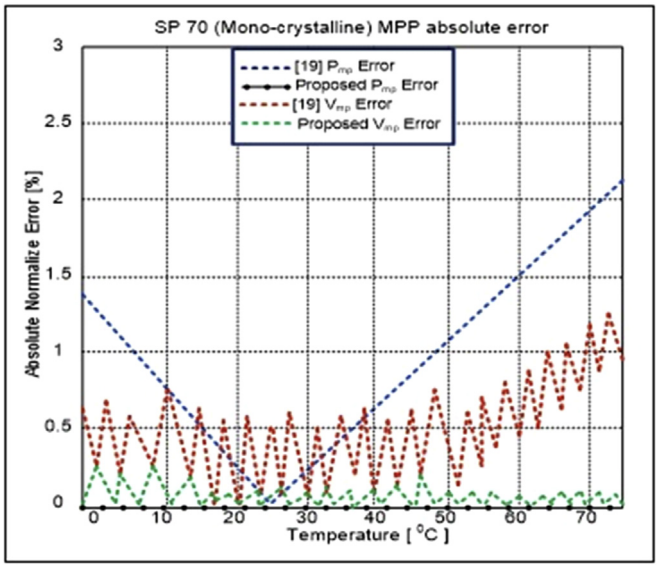

Fig. 13. Absolute error at MPP for SP-70 (Mono-crystalline) at different temperature, G = 1000 W/m^2, A.M = 1.5.

and P-V curves of KD210GH-2PU PV module at different insolation and temperature are obtained as shown in Figs. 10 and 11 respectively.

The circle marker at I_{sc}, P_{mp} and V_{oc} indicates manufacturer's experimental data and the results based on the proposed method are indicated by the solid lines. So, the proposed methodology and obtained results clearly indicate that the achieved characteristic curves are quite similar to the manufacturer's data, irrespective of varying atmospheric conditions.

4.3. Comparison of the proposed technique

In order to keep point of reference of the proposed technique with techniques used in Refs. [16] and [19], the relation between absolute error in power and voltage is shown in Fig. 12. It is seen that a similar range of accuracy is obtained between the presented method and method used in Ref. [19] for different values of temperature. The proposed method offers better accuracy at MPP, whereas, the method presented in Ref. [16], shows a considerable amount of error for different values of temperature.

By making the variations of 1 °C in the range of temperature from 0 °C to 75 °C, the findings based on two other PV modules (SP70 and SQ85) have also been observed. Fig. 13 illustrates the average result of SP70 PV module for 100 data sets.

Under STC, the error in results illustrated by model [19] is 0.013% for P_{mp} and 0.0515% for V_{mp} at MPP. As the temperature deviates from STC, accuracy decreases up to 2.73% and 2.11% at 0 °C and 75 °C temperature, respectively. Also variation of error in V_{mp} is observed at 0 °C–75 °C (mean = 0.573% and standard deviation = 0.289%).

In the present study, error of 0.001% for 'P_{mp}' and 0.10% for V_{mp} at STC are found. The maximum error 0.011% for P_{mp} is observed for specified temperature range and a standard deviation of 0.045 for V_{mp} is obtained. The obtained value is six times lower as compared to [19]. A similar pattern of results is obtained for SQ85 PV module. Table 6 gives the mean and standard deviation values for SP70 and SQ85 PV modules.

It is therefore recommended that in order to attain low modeling error under temperature variation, it is essential to adjust a, R_s and R_p.

5. Conclusions and future works

A novel approach of optimization technique based on PSO with binary constraints is presented in order to identify the unknown parameters of a single diode model. The proposed method completely eliminates the requirement of assuming the ideality factor. It also includes the temperature variations to identify the unknown parameters.

The evaluation of three different PV modules ensures the robustness of the proposed technique. The two novel approaches have been considered as a point of reference for the proposed technique. Appreciable accuracy in the results is achieved irrespective of temperature variations. The PSO algorithm has been executed 100 times with same initial condition as well as with standard parameter values provided by the manufacturer. The mean of maximum modeling error at MPP is found to be less than 0.02% for maximum voltage and 0.26% for maximum power.

In future, following works are proposed to improve the

Table 6
Comparison of absolute error at MPP (A.M 1.5, 1000 W/m^2).

Method	Shell SP70				Shell SQ85			
	Mean (%)		Standard Deviation (%)		Mean (%)		Standard Deviation (%)	
	P_{mp} Error	V_{mp} Error	P_{mp} Error	V_{mp} Error	P_{mp} Error	V_{mp} Error	P_{mp} Error	V_{mp} Error
[19]	1.246	0.573	0.726	0.289	1.373	0.420	0.829	0.282
Proposed	0.003	0.068	0.002	0.045	0.001	0.077	0.002	0.047

performance of PV model:

- With growing interests in the study of partial shading and accuracy concerns associated with low insolation and large PV installations, performance prediction is important for accurate energy yield. More elaborate and accurate models like two-diode model (or three-diode model) must be incorporated for performance analysis of the PV system.
- Further, one of the promising alternatives for computing the model parameters under these conditions could be hybrid approach.
- Furthermore, the PV models are still based on mono-crystalline and poly-crystalline technology. For instance, amorphous thin film modules have high ideality factor due to low fill factors. However, models presume fill factor in the range of $1 < a < 2$. There are very few committed efforts carried out for multi-junction, organic and dye synthesized PV cells. These are emerging areas of interests and particular problems related to them must be resolved.
- Finally, problems associated to cell degradations with time and weather conditions must be addressed. Additional coefficients can be added to mimic the cell deterioration for different module technologies. This effort will offer a greater understanding of the module performance over an extensive period of time.

Acknowledgement

This work was supported by Grant of Ministry of New and Renewable Energy (MNRE), Government of India and Indian Institute of Technology (IIT) Roorkee, Uttarakhand, India (Grant no. : 8793 38 061/429).

References

[1] D. Oliva, E. Cuevas, G. Pajares, Parameter identification of solar cells using artificial bee colony optimization, Energy 72 (2014) 93–102.
[2] Energy at the crossroads; 2015. ⟨http://home.cc.umanitoba.ca/~vsmil/pdf_pubs/oecd.pdf⟩.
[3] M. Buresch, Photovoltaic Energy System: Design and Installation, McGraw-Hill, New York, 1983, p. 335.
[4] Soon, T. Kok, Saad Mekhilef, A Fast-converging MPPT technique for photovoltaic system under fast varying solar irradiation and load resistance, IEEE Trans. Ind. Inf. 11 (1) (2015) 176–186.
[5] X. Weidong, W.G. Dunford, A. Capel, A novel modeling method for photovoltaic cells, in: 35th Annual Power Electronics Specialists Conference, 2004, PESC 04 2004, vol. 3, IEEE, 2004, pp. 1950–1956.
[6] N.N.B. Ulapane, C.H. Dhanapala, S.M. Wickramasinghe, S.G. Abeyratne, N. Rathnayake, P.J. Binduhewa, Extraction of parameters for simulating photovoltaic panels, in: 6th IEEE International Conference on Industrial and Information Systems (ICIIS), vol. 2011, 2011, pp. 539–544.
[7] R. Chenni, M. Makhlouf, T. Kerbache, A. Bouzid, A detailed modeling method for photovoltaic cells, Energy 32 (2007) 1724–1730.
[8] Q. Kou, S.A. Klein, W.A. Beckman, A method for estimating the long-term performance of direct-coupled PV pumping systems, Sol. Energy 64 (1998) 33–40.
[9] A. Bellini, S. Bifaretti, V. Iacovone, C. Cornaro, Simplified model of a photovoltaic module, in: Applied Electronics, 2009 AE 2009, IEEE, 2009, pp. 47–51.
[10] C.G. Moran, P. Arboleya, D. Reigosa, G. Diaz, J.G. Aleixandre, Improved model of photovoltaic sources considering ambient temperature and solar irradiation, in: Proc. IEEE PES/IAS Conf. Sustainable Alternative Energy, 2009, pp. 1–6.
[11] D. Kun, B. XinGao, L. HaiHao, P. Tao, A MATLAB-simulink-based PV module model and its application under conditions of non-uniform irradiance, IEEE Trans. Energy Convers. 27 (2012) 864–872.
[12] A.M. Humada, M. Hojabri, S. Mekhilef, H.M. Hamada, Solar cell parameters extraction based on single and double-diode models: a review, Renew. Sustain. Energy Rev. 56 (2016) 494–509.
[13] Kajihara, T. Harakawa, Model of photovoltaic cell circuits under partial shading, in: Proc. IEEE Int. Conf. Ind. Technol., 2005, pp. 866–870.
[14] Y.T. Tan, D.S. Kirschen, N. Jenkins, A model of PV generation suitable for stability analysis, IEEE Trans. Energy Convers. 19 (4) (Dec. 2004) 748–755.
[15] H. Altas, A.M. Sharaf, A photovoltaic array simulation model for MATLAB-simulink GUI environment, in: Proc. Int. Conf. Clean Elect. Power, 2007, pp. 341–345.
[16] E. Matagne, R. Chenni, Bachtiri R. El, A photovoltaic cell model based on nominal data only, in: Proc. Int. Conf. Power Eng., Energy Elect. Drives, 2007, pp. 562–565.
[17] W. Xiao, W.G. Dunford, A. Capel, A novel modeling method for photovoltaic cells, in: Proc. IEEE 35th Annu. Power Electron. Spec. Conf., vol. 3, 2004, pp. 1950–1956.
[18] G. Walker, Evaluating MPPT converter topologies using a MATLAB PV model, J. Elect. Electron. Eng. Aust. 21 (1) (2001) 45–55.
[19] M.G. Villalva, J.R. Gazoli, E.R. Filho, Comprehensive approach to modeling and simulation of photovoltaic arrays, IEEE Trans. Power Electron. 24 (5) (May 2009) 1198–1208.
[20] M. Bashahu, P. Nkundabakura, Review and tests of methods for the determination of the solar cell junction ideality factors, Sol. Energy 81 (2007) 856–863.
[21] A.T. Al-Awami, A. Zerguine, L. Cheded, A. Zidouri, W. Saif, A new modified particle swarm optimization algorithm for adaptive equalization, Digit. Signal Process. 21 (2) (Mar. 2011) 195–207.
[22] J.Y. Park, S.J. Choi, A novel datasheet-based parameter extraction method for a single-diode photovoltaic array model, Sol. Energy 122 (2015) 1235–1244.
[23] D. Jena, V.R. Ramana, Modeling of photovoltaic system for uniform and non-uniform irradiance: a critical review, Renew. Sustain. Energy Rev. 52 (2015) 400–417.
[24] J.K. Maherchandani, C. Agarwal, M. Sahi, Estimation of solar cell model parameter by hybrid genetic algorithm using MATLAB, Int. J. Adv. Res. Comput. Eng. Technol. 1 (6) (2012) 78–81.
[25] M. Zagrouba, A. Sellami, M. Boua, M. Ksouri, Identification of PV solar cells and modules parameters using the genetic algorithms: application to maximum power extraction, Sol. Energy 84 (2010) 860–866.
[26] S.J. Patel, A.K. Panchal, V. Kheraj, Solar cell parameters extraction from a current-voltage characteristic using genetic algorithm, J. Nano Electron. Phys. 5 (2) (2013) 5–7.
[27] K.M. El-Naggar, M.R. Al-Rashidi, M.F. Al-Hajri, A.K. Al-Othman, Simulated annealing algorithm for photovoltaic parameters identification, Sol. Energy 86 (2012) 266–274.
[28] Y. Shi, R. Eberhart, Parameter selection in particle swarm optimization, in: V.W. Porto, N. Saravanan, D. Waagen, A.E. Eiben (Eds.), Evolutionary Programming VII SE - 57, vol. 1447, Springer Berlin Heidelberg, 1998, pp. 591–600.
[29] A. Khare, S. Rangnekar, A review of particle swarm optimization and its applications in solar photovoltaic system, Appl. Soft Comput. J. 13 (5) (2013) 2997–3006.
[30] Q. Hengsi, J.W. Kimball, Parameter determination of photovoltaic cells from field testing data using particle swarm optimization, in: Power and Energy Conference at Illinois (PECI), 2011, IEEE, 2011, pp. 1–4.
[31] M. Ji, Z. Jin, H. Tang, An improved simulated annealing for solving the linear constrained optimization problems, Appl. Math. Comput. 183 (2006) 251–259.
[32] G. Zwe-Lee, A particle swarm optimization approach for optimum design of PID controller in AVR system, IEEE Trans. Energy Convers. 19 (2004) 384–391.
[33] J. Ma, T.O. Ting, K.L. Man, N. Zhang, S.-U. Guan, P.W.H. Wong, Parameter estimation of photovoltaic models via cuckoo search, J. Appl. Math. 2013 (2013) 8.
[34] A. Askarzadeh, A. Rezazadeh, Artificial bee swarm optimization algorithm for parameters identification of solar cell models, Appl. Energy 102 (2013) 943–949.
[35] N. Rajasekar, N.K. Kumar, R. Venugopalan, Bacterial foraging algorithm based solar PV parameter estimation, Sol. Energy 97 (2013) 255–265.
[36] H. Qin, J.W. Kimball, Parameter determination of photovoltaic cells from field testing data using particle swarm optimization, in: Proc. IEEE Power Energy Conf., 2011, pp. 1–4.
[37] H. Wei, J. Cong, X. Lingyun, S. Deyun, Extracting solar cell model parameters based on chaos particle swarm algorithm, in: International Conference on Electric Information and Control Engineering (ICEICE), IEEE, 2011, pp. 398–402.
[38] M. Ye, X. Wang, Y. Xu, Parameter extraction of solar cells using particle swarm optimization, J. Appl. Phys. 105 (2009) 094502.
[39] Y.A.N. Chun-man, G.U.O. Bao-long, W.U. Xian-xiang, Empirical study of the inertia weight particle swarm optimization with constraint factor, Int. J. Soft Comput. Softw. Eng. 2 (2) (2012) 1–8.
[40] X. Liang, Z. Yin, Y. Wang, Q. Sun, Impulse engine ignition algorithm based on genetic particle swarm optimization, in: Y. Tan, Y. Shi, H. Mo (Eds.), Advances in Swarm Intelligence SE - 5, vol. 7929, Springer Berlin Heidelberg, 2013, pp. 35–43.
[41] H. Bellia, Y. Ramdani, F. Moulay, A detailed modeling of photovoltaic module using MATLAB, NRIAG J. Astron. Geophys. 3 (2014) 53–61.
[42] Alain K. Tossa, Y.M. Soro, Y. Azoumah, D. Yamegueu, A new approach to estimate the performance and energy productivity of photovoltaic modules in real operating conditions, Sol. Energy 110 (2014) 543–560.
[43] W. Xiao, W.G. Dunford, A. Capel, A novel modeling method for photovoltaic cells, in: Proc. IEEE 35th Annu. Power Electron. Spec. Conf., vol. 3, 2004, pp. 1950–1956.
[44] D.H. Muhsen, A.B. Ghazali, T. Khatib, I.A. Abed, A comparative study of evolutionary algorithms and adapting control parameters for estimating the parameters of a single-diode photovoltaic module's model, Renew. Energy 96

(2016) 377–389.
[45] F.J. Toledo, J.M. Blanes, Analytical and quasi-explicit four arbitrary point method for extraction of solar cell single-diode model parameters, Renew. Energy 92 (2016) 346–356.
[46] C. Chellaswamy, R. Ramesh, Parameter extraction of solar cell models based on adaptive differential evolution algorithm, Renew. Energy 97 (2016) 823837.
[47] D.L. King, J.A. Kratochvil, W.E. Boyson, Temperature coefficients for PV modules and arrays: measurement methods, difficulties, and results, in: Proc. IEEE Photovoltaic. Spec. Conf., 1997, pp. 1183–1186.
[48] KD210GH-2PU High Efficiency Multi-crystalline Photovoltaic Module Datasheet. Kyocera. (2009).[Online].Available:http://www.kyocerasolar.de/index/products/download/English.cps_7724_files_8653File.cpsdownload.tmp/KD210GH2PU_Eng_January%202009.pdf.
[49] SP70 Photovoltaic Solar Module Datasheet. Shell Solar. [Online]. Available: http://telemetryhelp.com/Datasheets/ShellSP70_USv1.pdf.
[50] SP85-P/80-P Solar Modules for Off Grids Markets Datasheet. Shell Solar. (2004). [Online]. Available: http://www.effectivesolar.com/PDF/shell/SQ-80-85-P.pdf.